iJRASET
International Journal For Research in
Applied Science and Engineering Technology

INTERNATIONAL JOURNAL
FOR RESEARCH
IN APPLIED SCIENCE & ENGINEERING TECHNOLOGY

Volume: 13 Issue: VI Month of publication: June 2025

DOI: https://doi.org/10.22214/ijraset.2025.72511

International Journal for Research in Applied Science & Engineering Technology (IJRASET)
ISSN: 2321-9653; IC Value: 45.98; SJ Impact Factor: 7.538
Volume 13 Issue VI June 2025- Available at www.ijraset.com

A Hybrid Renewable Energy System (HRES) with a Proportional-Resonant (PR) Controlled Inverter

Dipak Khachane[1], Prof. M.F.A.R. Satarkar[2], Pankaj Banswal[3], Vaibhavi Bhostekar[4], Shubhankar Vadke[5]
[1, 3, 4, 5]*B-Tech Student, Department of Electrical Engineering, Dr. Babasaheb Ambedkar Technological University, Maharashtra, India*

***Abstract:** This paper investigates the effectiveness of Proportional-Resonant (PR) controllers in Hybrid Renewable Energy Systems (HRES), which integrate solar and wind components to optimize energy reliability and efficiency. The study addresses the research question regarding the extent to which PR controllers enhance performance and efficiency in managing power quality, system stability, and frequency-specific control in grid-connected applications. Experimental evaluations further validate that variations in load conditions, such as those from RL loads, have minimal impact on output performance, underscoring the robustness of the PR approach.*

Additionally, the development and testing of a small-scale hybrid wind-solar microgrid, including tailored power electronic converters, control algorithms, and an energy management system, illustrate the practical applicability of these advanced control strategies in both standalone and dynamic operational environments.

***Keywords:** hybrid system, standalone system, wind energy, Power quality, THD, Power Electronics, Renewable Energy.*

I. INTRODUCTION

The increasing global emphasis on sustainable energy independence has driven the adoption of hybrid renewable energy systems (HRES) that synergize multiple renewable sources, such as solar and wind, to mitigate intermittency and bolster reliability [1-2]. These systems are pivotal in achieving self-sufficient power generation, yet their performance hinges on sophisticated control strategies to manage dynamic interactions between energy sources, converters, and variable loads. While solar and wind energy dominate HRES configurations, their integration introduces challenges in power quality, stability, and frequency regulation, necessitating advanced control solutions [7-9].

Recent research has explored diverse control frameworks to address these challenges. For instance, simulations of hybrid systems under real-world load profiles and weather conditions underscore the importance of adaptive energy management [10]. Coordinated control architectures for standalone microgrids have also been proposed, emphasizing configurable systems that maintain power balance amid fluctuating generation and demand. Despite these advancements, gaps persist in optimizing harmonic suppression, frequency-specific precision, and resilience to load variations—critical factors for grid-connected applications. This study investigates the efficacy of Proportional-Resonant (PR) controllers in HRES, focusing on their ability to enhance power quality, stabilize grid interactions, and mitigate frequency deviations. Experimental validation is conducted using a small-scale hybrid wind-solar microgrid equipped with customized power electronic converters and an adaptive energy management system. The results demonstrate the robustness of PR controllers in maintaining consistent output performance under resistive-inductive (RL) load fluctuations, highlighting their suitability for both standalone and grid-tied environments. By bridging theoretical insights with practical implementation, this work advances scalable control strategies for HRES, contributing to the global transition toward resilient and efficient renewable energy systems.

II. SYSTEM DESCRIPTION

The proposed system is shown in Fig. 1. It can be divided into Two parts; i) solar and wind based renewable energy sources along with their converters connected to the DC bus, ii) the load side inverter and single-phase load, iii) real time controller implementing the PR controller system. The wind energy conversion system consists of a permanent magnet synchronous generator (PMSG) based wind turbine and solar photovoltaic (PV) panel.

An energy management system is used to control the power flow under different conditions in order to supply to the load through a single-phase inverter.

A. Solar Energy Conversion System (SECS)

The SECS consists of a solar PV panel, a DC-DC boost converter with closed loop PI controller The P-V characteristics of the solar panel with effect of irradiance. The characteristics are shown for different values of irradiance ranging from 1500W/m2 to 600W/m2 at a constant temperature of 250C.

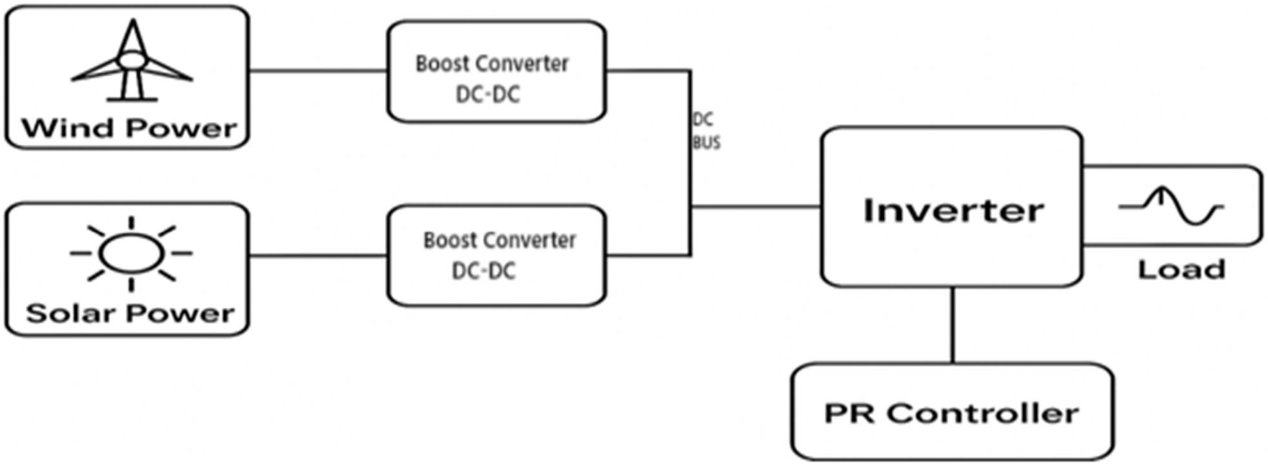

Fig 1. Components of small-scale wind-solar microgrid with controlled converters

B. Wind Energy Conversion System (WECS)

The WECS consists of a wind turbine, a PMSG, a DC-DC boost converter and controller. The power extracted from the wind is...

$$P_m = \frac{1}{2} C_p(\lambda, \beta)\rho \times A \times V\omega^3 \quad \ldots (1)$$

where ρ is the air density in kg/m^3, A is the area swept by the rotor blades in m^2, and Vw is the wind velocity in m/s. Cp is the power coefficient and is a function of tip speed ratio (TSR, λ) and blade pitch angle (β). A variable speed wind turbine is used in this system. the Cp for various wind speeds at different pitch angles. A permanent magnet synchronous generator is selected for its low maintenance and low operational cost. The generator output is dependent on the wind speed. The three-phase output of the generator is rectified using a diode rectifier and then the voltage level is increased with the help of a DC-DC boost converter.

$$C_p(\lambda, \beta) = C_1\left(\frac{C_2}{\lambda_i} - C_3\beta - C_4 \times \beta^x - C_5\right) exp\left(-\frac{C_6}{\lambda_i}\right)$$

$$C_p = 0.41034 \quad \ldots (2)$$

Where C_1.........C_6 are constant

$$\frac{1}{\lambda_i} = \frac{1}{\lambda + 0.08\beta} - \frac{0.035}{1 + \beta^2}$$

$$\lambda_i = 11.304 \quad \ldots (3)$$

$$\lambda = \frac{\omega_r}{V_\omega}$$

$$\omega_r = 25.07$$

$$\lambda = 8.1 \quad \ldots (4)$$

where,

C_{popt} (λ, β) =0.41

V_m=12m/sec

R=3.877

$C_1, C_2, C_3, C_4, C_5, C_6$ = 0.5,116,0.4,0.5.21

International Journal for Research in Applied Science & Engineering Technology (IJRASET)
ISSN: 2321-9653; IC Value: 45.98; SJ Impact Factor: 7.538
Volume 13 Issue VI June 2025- Available at www.ijraset.com

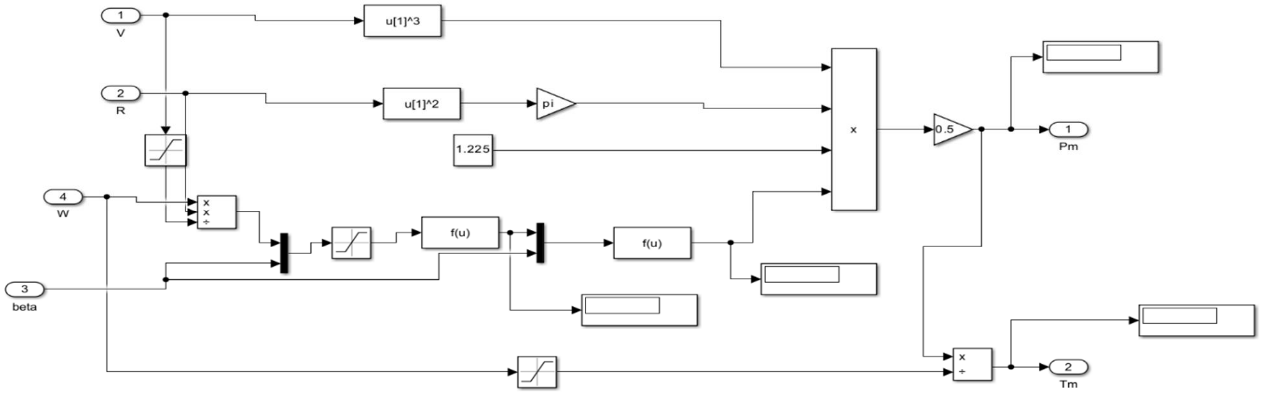

Fig 2. Mathematical modelling of wind power plant.

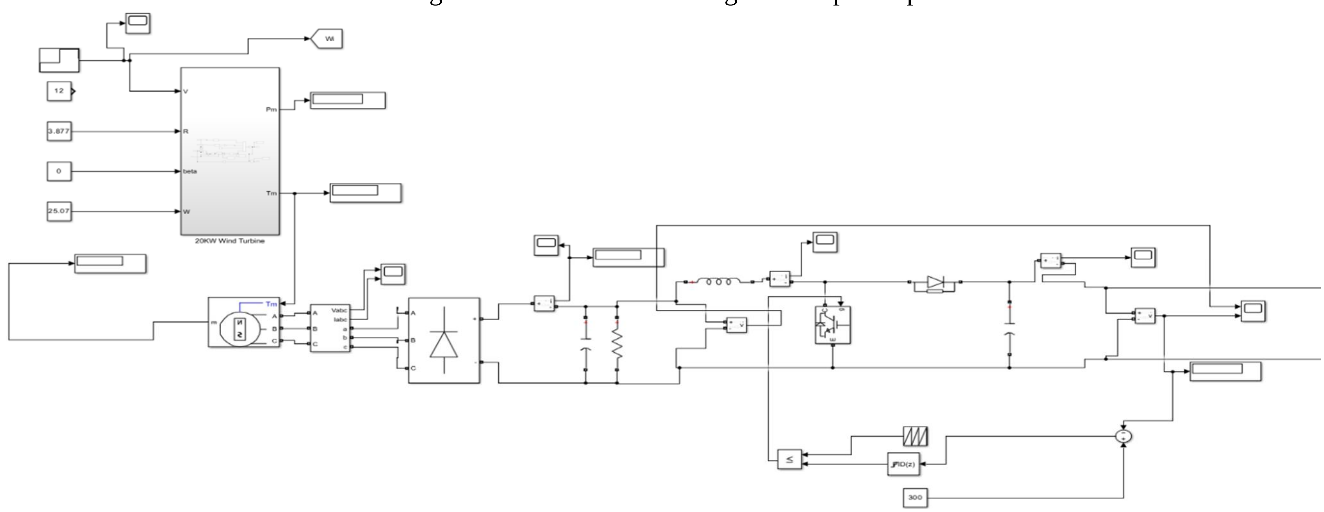

Fig 3. Wind energy conversion system with controller.

C. Load Side Control

The DC microgrid is connected to a single-phase resistive load through a single-phase inverter with a controller shown in Fig. 4. A R-L filter is used at the inverter output to filter the undesired harmonic content. The outer loop PI controller is used to regulate the voltage and the inner loop PR controller regulates the current.

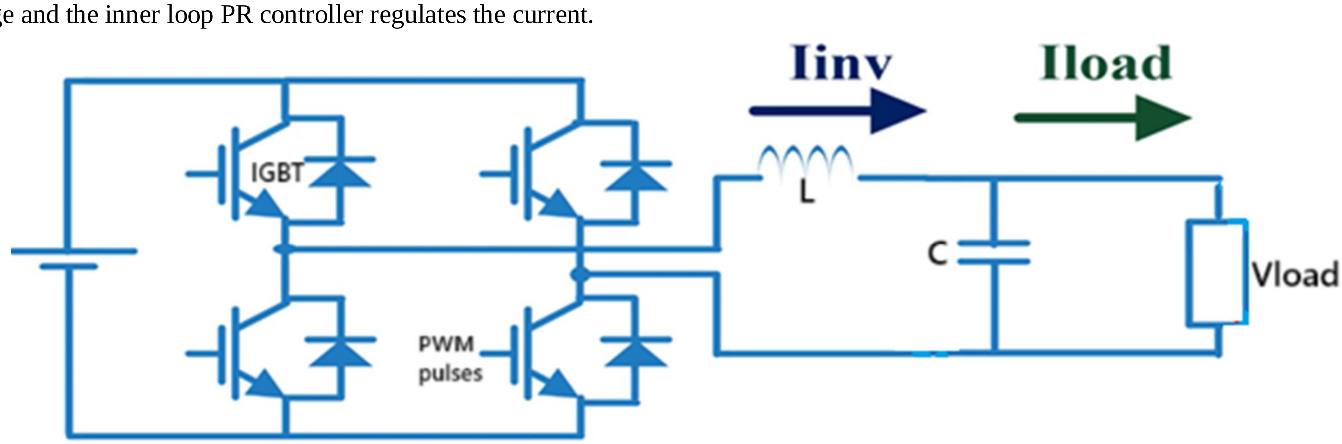

Fig 4. Single phase inverter with filter for AC load control.

Table 1: Comparison of Solar, Wind, and Hybrid Power Systems

Feature	Solar Power System	Wind Power System	Solar-Wind Hybrid System
Energy Reliability	Moderate (only in sunlight)	Moderate (only in windy conditions)	High (complementary energy sources)
Power Fluctuations	High (affected by weather)	High (affected by wind speed)	Low (balanced by hybridization)
Grid Independence	Limited	Limited	High
Cost Effectiveness	Medium	Medium	High (due to optimized utilization)
Environmental Impact	Low	Low	Very Low
Maintenance Complexity	Low	High (moving parts in wind turbine)	Medium
Best Application	Sunny regions	Windy regions	Areas with mixed solar and wind potential

Table energy highlights the superiority of the hybrid power system in terms of credibility, low fluctuations, cost -effectiveness and stability. The ability to utilize energy from both sources reduces the storage requirements and reduces the dependence on backup. In addition, artificial intelligence (AI) -co -working management systems, real -time seasons and smart network integration improves further efficiency of technological progress and hybrid renewable energy systems. The real applications of the Solar-Hwa hybrid system are different and grow rapidly. These systems are used to provide power to remote areas for electrification of the countryside where network connection is limited. They are also used extensively in the telecommunications towers which ensure an uninterrupted power supply to the communication network. Industrial and commercial companies use hybrid power solutions to reduce operating costs and reduce carbon footprint.

D. Proportional Resonant Pr Controller

Kp Value

1. Voltage Controller
- Controller Time Constant = 200 µs
- Filter Capacitance = 6.23 µF

Calculation:

$$K_p = \frac{capacitance}{Time\ Constant} = \frac{6.23\mu f}{200\mu s} = 0.03115$$

2. Current Controller
- Controller Time Constant = 150 µs
- Filter Inductance = 4.06 mH

Calculation:

$$K_p = \frac{Inductance}{Time\ Constant} = \frac{4.06mH}{150\mu s} = 27.066$$

Kr Value

$$G_n = \frac{kr.\omega n}{\omega n^2.\omega^2}$$

1. Voltage Controller
- Kr Value of voltage controller is =100

$$\frac{\omega^2}{Kr} = \left(\frac{2 \times Pi \times 50}{100}\right)^2 = 986.83$$

2. Current Controller

• Kr Value of Current controller is =400

$$\frac{\omega^2}{Kr} = \left(\frac{2 \times Pi \times 50}{400}\right)^2 = 246.7$$

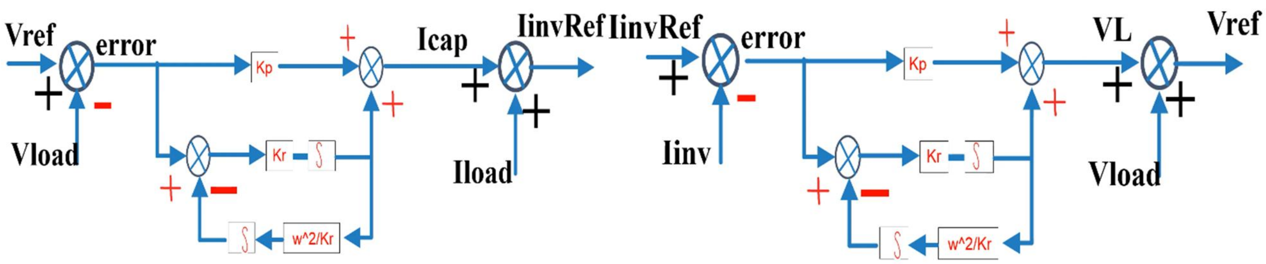

Fig 5. Proportional Resonant Controller

Standalone inverters are critical in off-grid renewable energy applications, enabling stable AC power delivery to local loads. A central challenge in standalone inverter design is maintaining power quality under dynamic load variations. To address this, Proportional-Resonant (PR) controllers are preferred over PI controllers due to their superior tracking performance for sinusoidal references. [3]

1. System Overview The control system is implemented in two cascaded loops:

- An outer voltage control loop to regulate the output AC voltage.
- An inner current control loop to manage inverter output current.

Each loop is implemented using a PR controller for enhanced frequency response and steady-state accuracy.

2. Voltage Control Loop Design

The reference voltage is compared with the actual load voltage, producing an error signal:

$$\text{Error} = V_{ref} - V_{load}$$

The error signal is fed into a PR controller which processes it to generate a control signal equivalent to the required capacitor current.

$$I_{CAP} = PR_v(\text{error})$$

The total inverter current reference is calculated by adding the capacitor current and the load current.

$$I_{inv.ref} = I_{CAP} + I_{load}$$

This summation is based on Kirchhoff's Current Law (KCL).

3. Current Control Loop Design

The reference inverter current is compared with the actual inverter current.

$$\text{Error} = I_{inv.ref} - I_{inv}$$

The resulting error is processed by the current loop PR controller, yielding the required inductor voltage.

$$V_L = PR_i(\text{error})$$

Using Kirchhoff's Voltage Law (KVL), the inverter output voltage reference is derived by summing the inductor voltage with the load voltage.

$$I_{inv.ref} = V_L + V_{load}$$

The reference voltage is used as the input for the PWM generation block, which synthesizes the output waveform.

III.SIMULATION AND RESULT

In this Simulink model, a hybrid renewable energy system combining variable solar and wind energy sources is modelled in MATLAB/Simulink. The variable DC outputs from photovoltaic and wind energy conversion systems are integrated and fed into a closed-loop boost converter. The converter is designed to stabilize the DC bus voltage at 250 V under fluctuating environmental conditions. The regulated DC voltage is then supplied to a full-bridge voltage-source inverter (VSI) controlled using a Proportional-Resonant (PR) controller.

The PR control strategy ensures accurate sinusoidal voltage generation with minimal steady-state error at the fundamental frequency. The inverter output is connected to a variable DC load, and the system performance is evaluated in terms of output voltage stability, Total Harmonic Distortion (THD), and power factor. Simulation results demonstrate that the proposed control system achieves acceptable THD levels (within IEEE 519 standards) and maintains a power factor close to unity, ensuring high-quality power delivery and efficient operation under varying generation and loading conditions.

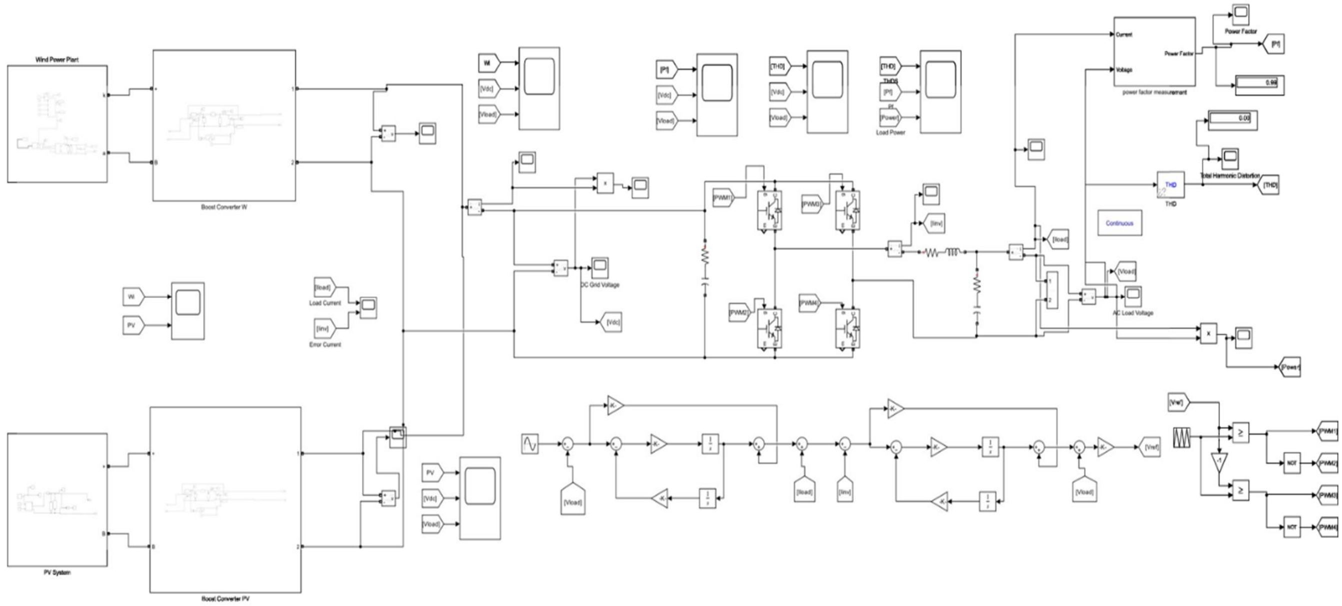

Fig 6. Simulink Model

A. Experimental Results

A single case scenario was simulated, in which both the renewable energy inputs and the load were varied to assess the system's dynamic performance. Stepped variations in solar and wind generation were introduced using a Stair Generator, and the load demand was simultaneously changed during the 3-second simulation runtime.

The results show that the system successfully maintained a stable DC voltage output and achieved acceptable levels of Total Harmonic Distortion (THD) and power factor, validating the effectiveness of the control strategies used.

Case Study Objective with Real-Time Data Inputs

The objective of this case is to deliver real-time power to a variable load under fluctuating solar and wind generation, without the use of any energy storage system.

The solar irradiance is varied over time to replicate changing sunlight conditions, similar to using controlled artificial lighting. The irradiance values at time intervals of 0, 0.5, 1, 1.5, 2, and 2.5 seconds are 50 W/m², 700 W/m², 1000 W/m², 700 W/m², 600 W/m², and 500 W/m², respectively.

Simultaneously, the wind speed varies at the same time intervals to mimic dynamic wind conditions, such as those produced by a variable-speed fan. The wind speed values are 6 m/s, 7 m/s, 8 m/s, 10 m/s, 9 m/s, and 8 m/s at 0, 0.5, 1, 1.5, 2, and 2.5 seconds, respectively.

Unlike many studies that assume a fixed load or include a battery for energy balancing, this simulation includes a variable load and no battery or energy storage system. The load values over time are 7 kW, 17 kW, 12 kW, 25 kW, 20 kW, and 15 kW, respectively. This configuration makes the system more challenging, as all generated power must meet the instantaneous load demand.

Although the variations in solar irradiance and wind speed are modelled as step changes—which rarely occur in real-world scenarios—this method is effective for evaluating system response to sudden fluctuations. The input values span the practical operating range of both the photovoltaic (PV) system and wind turbine (WT), allowing assessment of their combined performance.

This case study helps demonstrate how a hybrid renewable energy system without energy storage responds to simultaneous variations in both generation and load, reflecting a more realistic and demanding operational scenario.

Table 2: Case Study Objective with Real-Time Data Inputs

Sr. no.	Time (s)	Load (kw)	Solar irradiance (w/m^2)	Wind speed (m/s)	Power factor	Total Harmonic Distortion	Total consumed Power (w)	Current (Amp)
1	0-0.5	7	50	6	0.92	0.03	6500	40
2	0.5-1	17	700	7	0.96	0.03	16700	65
3	1-1.5	12	1000	8	0.98	0.01	12000	50
4	1.5-2	25	700	10	0.98	0.01	23500	102
5	2-2.5	20	600	9	0.95	0.02	18000	80
6	2.5-3	15	500	8	0.98	0.01	13500	60

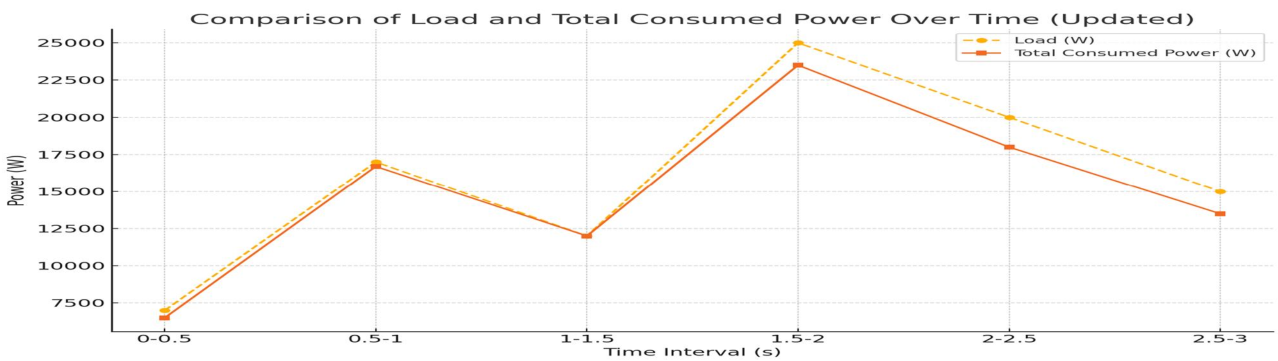

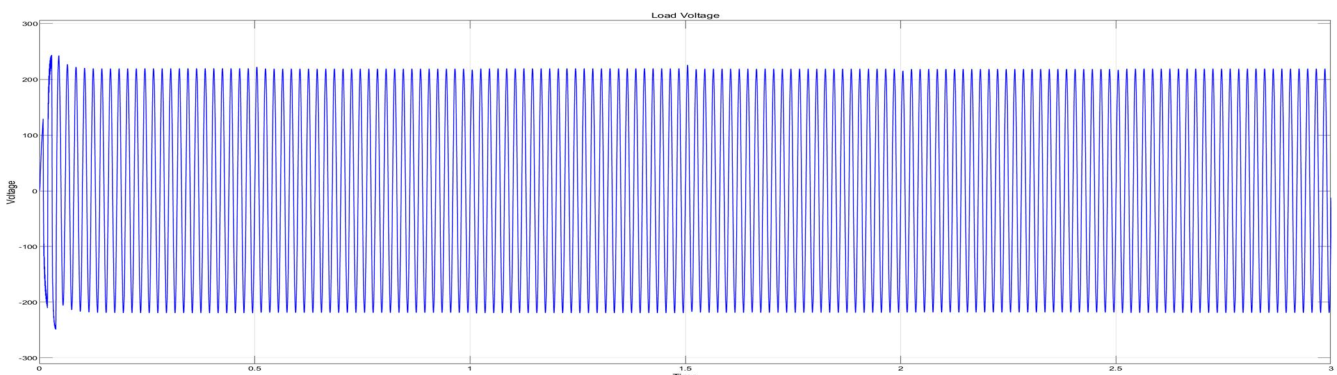

Fig 7. Load Voltage.

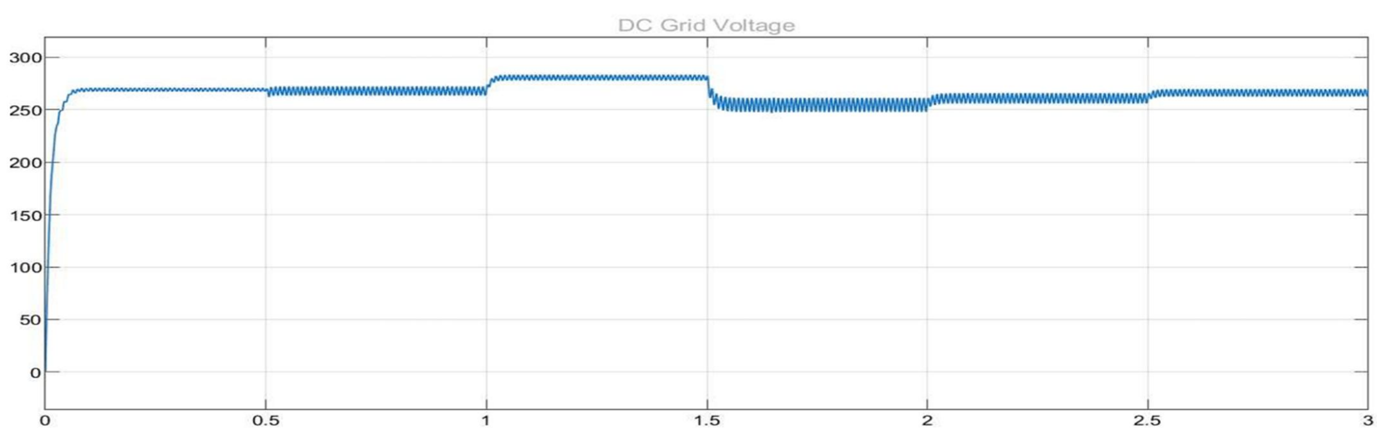

Fig 8. DC Bus Voltage for variable load with variable RES.

International Journal for Research in Applied Science & Engineering Technology (IJRASET)
ISSN: 2321-9653; IC Value: 45.98; SJ Impact Factor: 7.538
Volume 13 Issue VI June 2025- Available at www.ijraset.com

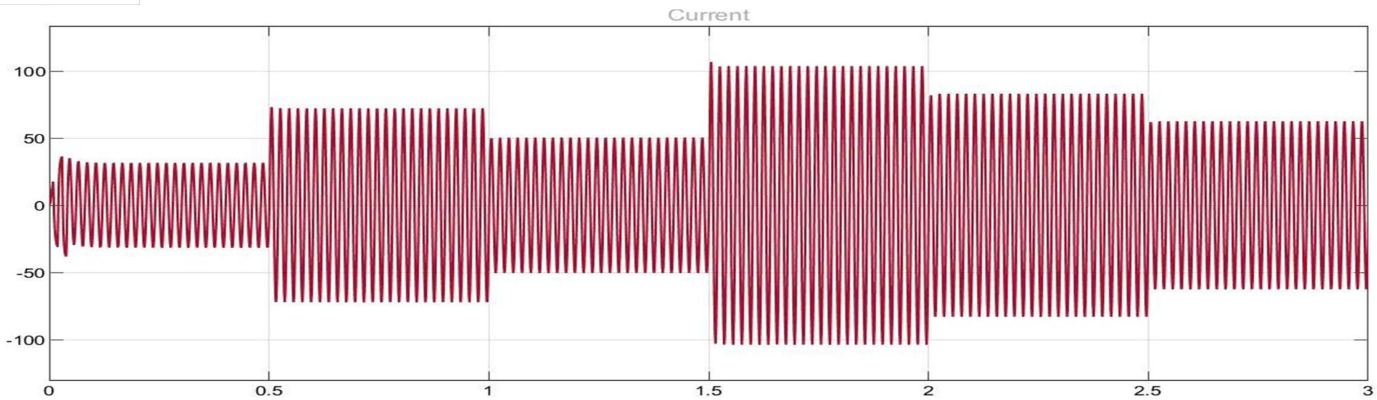

Fig 9. Inverter O/P Current

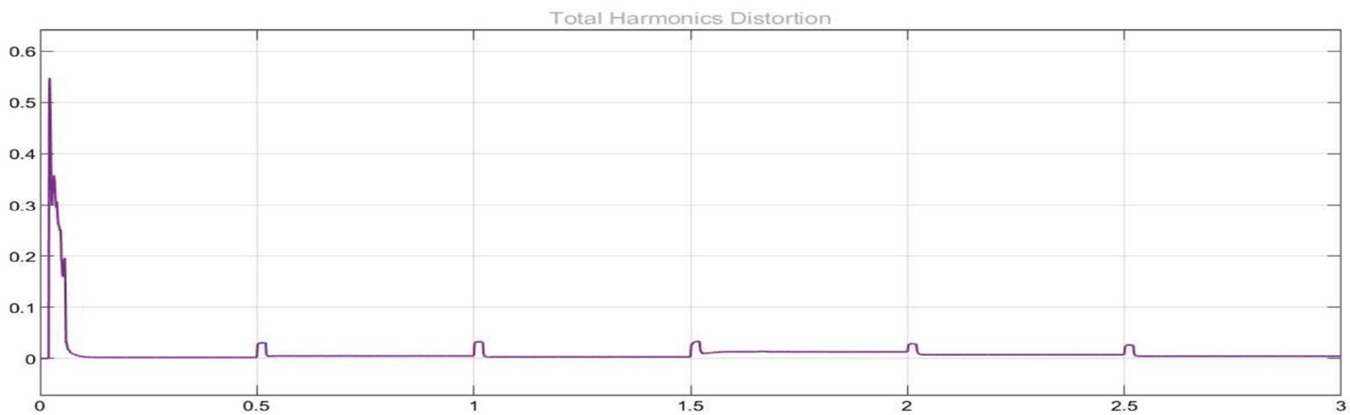

Fig 10. Total Harmonics Distortions of System

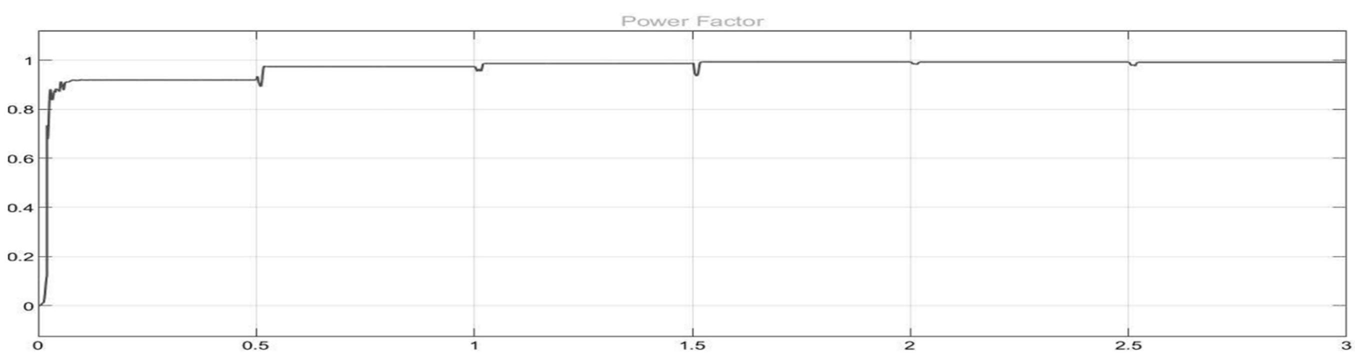

Fig 11. Power Factor of System

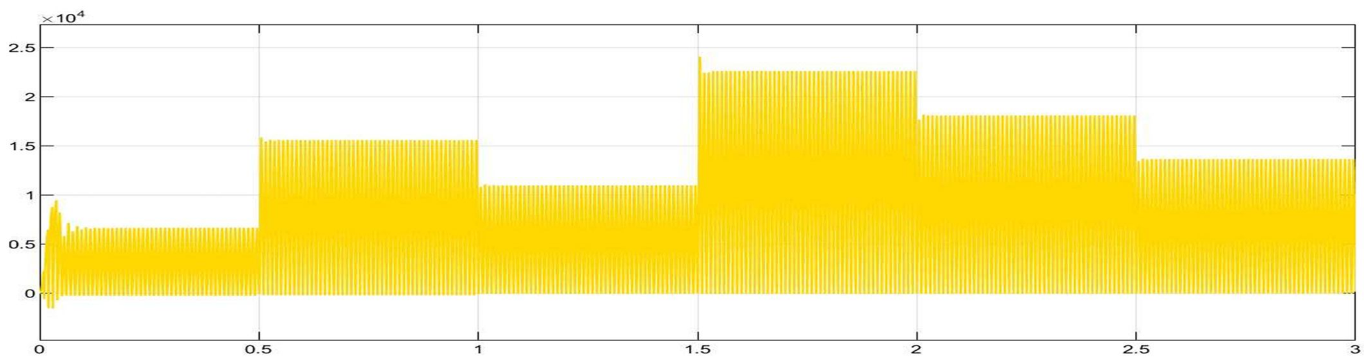

Fig 12. Power Consumed by load

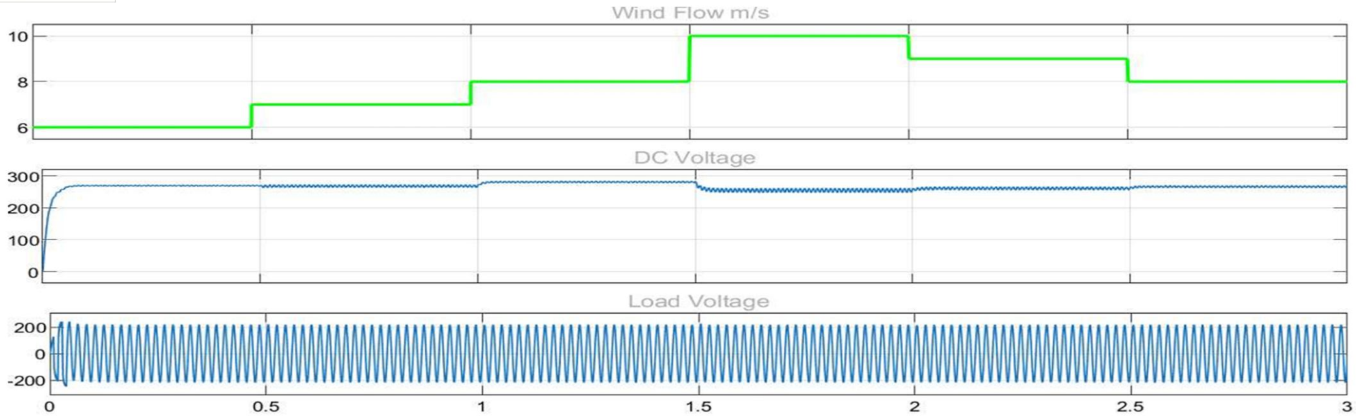

Fig 13. Variable wind I/P and Inverter load voltage

Top plot: This represents the wind speed input (in m/s), which varies in a stepwise manner from 6 m/s to 8 m/s at 1 second, and then to 11 m/s at 2 seconds. These steps simulate real-world wind speed variations.

Middle plot: This shows the DC bus voltage. The voltage quickly rises and stabilizes around 280 V. During wind speed changes, minor fluctuations occur but the voltage quickly returns to its steady-state value, indicating effective voltage regulation.

Bottom plot: This displays the AC load voltage. Despite the changes in wind speed and load conditions, the inverter output remains a stable sinusoidal waveform, maintaining constant amplitude and frequency throughout the simulation.

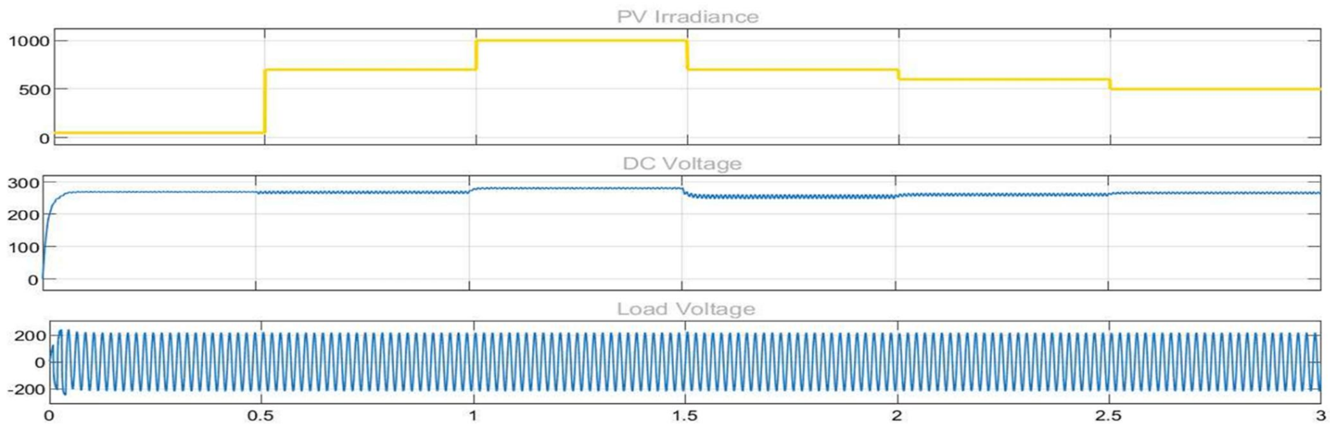

Fig 14. Variable Irradiance I/P and Inverter load voltage

Top plot: The solar irradiance (in W/m²) varies in a stepwise manner from 0 to 800 W/m² at 1 second, and then to 1000 W/m² at 2 seconds. This simulates realistic changes in solar input during the day.

Middle plot: The DC bus voltage remains nearly constant around 280 V throughout the simulation. Despite the changes in irradiance, only small transient dips are observed, indicating effective voltage regulation and MPPT operation.

Bottom plot: The inverter output maintains a steady sinusoidal AC voltage waveform, showing that the system consistently supplies a stable load voltage regardless of changes in solar input and load variation.

IV. CONCLUSIONS

A simulation model of a hybrid solar–wind energy system was successfully developed to reflect real-world scenarios involving variable renewable inputs and dynamic load demands. The system employs a closed-loop PI-controlled DC-DC boost converter to regulate the DC bus voltage under fluctuating wind and solar power inputs. This regulated DC voltage is then converted to AC using a PR-controlled inverter, which supplies power to a variable load.

The simulation results confirm that the system maintains a stable DC bus and steady AC output, demonstrating effective handling of practical variations. The Total Harmonic Distortion (THD) of the inverter output voltage was found to be within acceptable limits—typically less than 5%, as recommended by IEEE Standard 519. The Power Factor (PF) of the system remained high—above 0.95, which is generally considered acceptable for grid-connected and standalone applications.

These results validate the effectiveness of the chosen control strategies and confirm the system's capability to operate efficiently under dynamic real-life conditions. This work offers a foundation for further development, real-time implementation, and testing of hybrid renewable energy systems.

V. ACKNOWLEDGMENT

We would like to express our sincere gratitude to Prof. M. F. A. R. Satarkar, our project guide, for his invaluable guidance, support, and encouragement throughout the development of this project. His expertise and feedback played a crucial role in shaping the direction and outcome of our work.

We also extend our thanks to the Department of Electrical Engineering for providing the necessary facilities and academic environment that enabled us to complete this project successfully.

This project was carried out by Dipak Khachane along with three dedicated team members, whose collaboration and teamwork were essential to the successful completion of this work.

Finally, we are thankful to our families and friends for their constant support and motivation throughout this journey.

REFERENCES

[1] Atika Qazi et al., “Towards Sustainable Energy: A Systematic Review of Renewable Energy Sources, Technologies, and Public Opinions”, IEEE Access, vol. 7, pp. 63837 – 63851, May, 2019..

[2] Trieu Mai et al., “Renewable Electricity Futures for the United States” IEEE Trans. on Sustainable Energy, vol. 5, no. 2, pp. 372-378, Apr. 2014.

[3] Teodorescu, R., Liserre, M., & Rodriguez, P. (2011). Grid Converters for Photovoltaic and Wind Power Systems. Wiley.

[4] Saroja Kanti Sahoo et al., “Control Techniques in AC, DC, and Hybrid AC–DC Microgrid: A Review”, IEEE Journal of Emerging and Selected Topics in Power Electronics, vol. 6, iss. 2, pp. 738–759, Jun. 2018.

[5] Ahmed, S., & Nayar, C. V. (2020). Hybrid renewable energy systems: Optimization and control. Renewable Energy, 150, 620-634.

[6] Caisheng Wang et al., “From hybrid energy systems to microgrids: Hybridization techniques, configuration, and control”, IEEE PES General Meeting, USA, pp. 1-4, Jul. 2010.

[7] Saroja Kanti Sahoo et al., “Control Techniques in AC, DC, and Hybrid AC–DC Microgrid: A Review”, IEEE Journal of Emerging and Selected Topics in Power Electronics, vol. 6, iss. 2, pp. 738–759, Jun. 2018.

[8] Venkata Yaramasu et al., “High-power wind energy conversion systems: State-of-the-art and emerging technologies”, Proceedings of the IEEE, vol. 103, iss. 5, pp. 740–788, May, 2015.

[9] Caisheng Wang and M. Hashem Nehrir, “Power Management of a Stand-Alone Wind/Photovoltaic/Fuel Cell Energy System”, IEEE Trans. Energy Conversion, vol. 23, no. 3, pp. 957-967, Sept. 2008.

[10] Blaabjerg, F., & Ma, K. (2021). Future trends in power electronics for renewable energy systems. IEEE Journal of Emerging and Selected Topics in Power Electronics, 9(2), 964-976.

[11] https://in.mathworks.com/matlabcentral/fileexchange/128213-hybrid-renewable-energy-system

[12] Karimi, M., & Yazdani, A. (2021). Inverter-based renewable energy integration. IEEE Transactions on Energy Conversion, 36(3), 2101-2112.

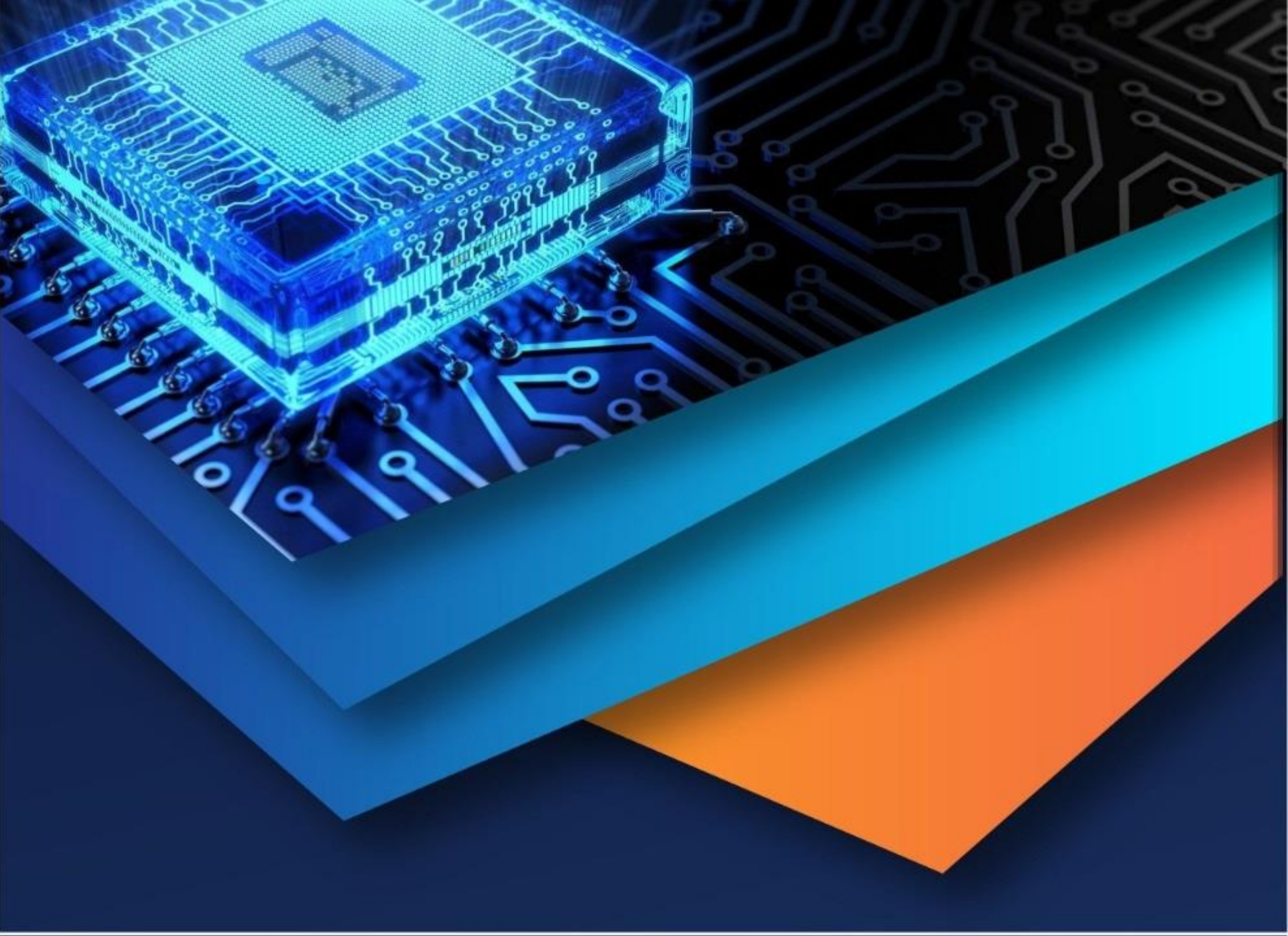

10.22214/IJRASET

45.98

IMPACT FACTOR: 7.129

IMPACT FACTOR: 7.429